This is an *Accepted Manuscript*, which has been through the Royal Society of Chemistry peer review process and has been accepted for publication.

Accepted Manuscripts are published online shortly after acceptance, before technical editing, formatting and proof reading. Using this free service, authors can make their results available to the community, in citable form, before we publish the edited article. We will replace this *Accepted Manuscript* with the edited and formatted *Advance Article* as soon as it is available.

You can find more information about *Accepted Manuscripts* in the **Information for Authors**.

Please note that technical editing may introduce minor changes to the text and/or graphics, which may alter content. The journal's standard **Terms & Conditions** and the **Ethical guidelines** still apply. In no event shall the Royal Society of Chemistry be held responsible for any errors or omissions in this *Accepted Manuscript* or any consequences arising from the use of any information it contains.

Indicator displacement assay for cholesterol electrochemical sensing using

calix[6]arene functionalized graphene-modified electrode

Long Yang[a, 1], Hui Zhao[b, 1], Yucong Li[a], Xin Ran[a], Guogang Deng[a], Yanqiong Zhang[a],

Hanzhang Ye[a], Genfu Zhao[a], Can-Peng Li[a, *]

[a] School of Chemical Science and Technology, Yunnan University, Kunming 650091,

PR China.

[b] Laboratory for Conservation and Utilization of Bio-resource, Yunnan University,

Kunming 650091, PR China.

[1]These authors contributed equally to this work.

* Corresponding authors.

Fax or Tel: 86-871-65031119. E-mail: lcppp1974@sina.com (C.-P. Li)

Abstract: A novel electrochemical method has been developed towards cholesterol detection based on competitive host–guest interaction by selecting methylene blue (MB) and calix[6]arene functionalized graphene (CX6-Gra) as the "reporter pair". Upon the presence of cholesterol to the performed CX6-Gra·MB complex, the MB molecules are displaced by cholesterol, leading to a "switch off" electrochemical response. A linear response range of 0.50 to 50.00 μM for cholesterol with a low detection limit of 0.20 μM (*S/N*=3) was obtained by using the proposed method. This method could be successfully utilized to detect cholesterol in serum samples, and may be expanded to analysis of other non-electroactive species. Besides, the host–guest interaction between cholesterol and CX6 was studied by molecular modeling calculations, which revealed that the complexation could reduce the energy of the system and the complex of 1:1 host–guest stoichiometry had the lowest binding free energy of −8.01 kcal/mol. In addition, the constructed electrochemical sensing platform is important as it does not use any enzyme or antibody for detection of cholesterol efficiently and selectively over the common interfering species.

Introduction

The concept of indicator displacement assay (IDA) has received considerable interest with the development of supramolecular chemistry, which exploit the potential of artificial receptors, particularly macrocyclic hosts, for its promising applications in molecular recognition and sensing. [1,2] The sensing principle of IDA relies on the competition between a test substance and an indicator for the same binding site on the

2

host. [3] When an analyte is added to a solution containing host·indicator complex, the

analyte displaces the indicator from the binding site. Upon displacement of the

indicator, a change in signal is observed. Although the IDA has been widely applied in

the fluorescent sensing filed, [4−10] it is rarely investigated for electrochemical sensing

applications except few researchers contributed to this area by using natural

β-cyclodextrin as macrocyclic host. [11−13]

Calixarenes, recognised as the third class of macrocyclic host molecules after

crown ethers and cyclodextrins, have become important receptors because they can

form stable host−guest complexes with various organic, inorganic, and biological

guest molecules, which show high supramolecular recognition and enrichment

capability. [14,15] Water-soluble calixarenes, particularly, p-sulfonated derivatives, have

been widely investigated to develop different electrochemical sensing platforms and

separation matrices due to their benign biocompatibility and simplicity of synthesis.

[10,16] Graphene is a material that holds great promise for potential applications in many

technological fields because of its extraordinary thermal, mechanical, and electrical

properties. [17] However, preparation of soluble graphene is challenging as graphene is

known to have poor solubility. [18] The advantage of water-soluble calixarenes as well

as cyclodextrins functionalization is that it offers high water solubility to graphene

and guest molecules incorporated into calixarenes are easily accessible to graphene. [16]

It has been reported that the composites of calixarenes and carbon materials (e.g.

carbon nanotube, graphene) could be formed by π−π interactions and hydrogen

interactions. [16,19−21] If graphene is modified with water-soluble calixarenes, it is likely

to gain new materials simultaneously possessing the large surface area and good

conductivity of graphene and high supramolecular recognition and enrichment

capability of calixarenes. Therefore, the integration of graphene and water-soluble

calixarenes can be potentially applied in the field of electrochemical sensing or

biosensing, and thus arouse extensive research interest.

Cholesterol is a vital component in cells and tissues of humans, playing a

functional role in construction of cell membranes or serving as a biosynthetic

precursor of bile acids, vitamin D, steroid hormones etc. [22] The normal level of total

cholesterol in healthy human serum is ~200 mg dL^{-1}. [23] Excess cholesterol in blood

serum forms plaques in the arteries of blood vessels which prevent the blood

circulation and cause cardiovascular diseases. [9] Thus the levels of total cholesterol in

serum and food are major parameters for diagnostic treatment. Herein, a sensitive and

selective electrochemical approach for cholesterol sensing based on a competitive

host-guest recognition between CX6 and signal probe/target molecules using

CX6-Gra modified electrode was developed for the first time. Methylene blue (MB)

and cholesterol were selected as the probe and target molecules, respectively. Due to

the host–guest interaction, MB molecules can enter into the hydrophobic inner cavity

of CX6, and the CX6-Gra modified glassy carbon electrode displays a remarkable

cathodic peak. In the presence of cholesterol, competitive interaction to CX6 occurs

and the MB molecules are displaced by cholesterol. This results in a decreased

reduction peak current of MB. As MB is a well-known redox probe and hence can be

easily detected using differential pulse voltammetery (DPV) technique.

Materials and methods

Chemicals and materials

Graphite oxide was purchased from Nanjing XFNANO Materials Tech Co., Ltd.

(Nanjing, China). 4-Sulfocalix[6]arene hydrate (CX6) was obtained from Tokyo

Chemical Industry Co., Ltd. (Tokyo, Japan). Corticosterone, estrone, β-estradiol, and

β-sitosterol were obtained from Shanghai Adamas Reagent Co., Ltd (Shanghai,

China). All other reagents were of analytical grade. Phosphate buffer (PBS, 0.1 M, pH

7.0) prepared by mixing stock solutions of 0.1 M KH_2PO_4 and K_2HPO_4 used as

working solution. All aqueous solutions were prepared with deionized water (DW, 18

$M\Omega$ cm).

Apparatus

Differential pulse voltammetery (DPV) and electrochemical impedance spectroscopy

(EIS) experiments were performed with a CHI 660E Electrochemical Workstation

from Shanghai Chenhua Instrument (Shanghai, China) and conducted using a

three-electrode system, with the modified GCE as working electrode, a platinum wire

as the counter electrode, a saturated calomel electrode (SCE) as the reference

electrode. The morphology of the prepared sample was characterized by a QUNT200

scanning electron microscopy (SEM, Hillsboro, Oregon, USA) and a JEM 2100

transmission electron microscopy (TEM, Tokyo, Japan). UV–visible spectra were

analyzed in a U-2001 Hitachi (Tokyo, Japan) UV spectrophotometer. Raman spectra

were obtained on a 400F PERKINELMER Raman spectrometer (Shelton, USA) with

514.5 nm wavelength incident laser light. Fluorescence titration experiments were

carried out using a Hitachi F–4500 fluorescence spectrophotometer (Tokyo, Japan) at

room temperature. Fourier transform infrared (FTIR) study was performed over the

wavenumber, range of 4000–400 cm^{-1} by a Thermo Fisher SCIENTIFIC Nicolet IS10

(Massachusetts, USA) FTIR impact 410 spectrophotometer using KBr pellets.

Thermogravimetric analysis (TGA) was carried out on a Q50 TGA (TA Instruments,

New Castle, Delaware, USA), from 25 to 800 ^{o}C at a heating rate of 5 ^{o}C min^{-1} in

argon.

Absorbance and fluorescence titration experiments

A stock solution of MB (500 μM) and a stock solution of CX6 (500 μM) in 0.1 M

PBS (pH 7.0) were prepared. As cholesterol has very low solubility in water, 500 μM

stock solution of cholesterol was prepared in ethanol. The dye stock solution was

diluted with 0.1 M PBS (pH 7.0) to a final concentration of 10 μM. CX6 was then

gradually added into the MB solution and mixed by vortexing well for 5 min before

the absorbance or fluorescence was recorded. For the competitive displacement of

MB from the CX6 by cholesterol, the required amount of cholesterol was gradually

added into the mixture of CX6 and MB and mixed by vortexing well for 5 min before

the absorbance or fluorescence was recorded.

Molecular docking

6

The crystal structures of 4-sulfocalix[6]arene hydrate (CX6) (ID: FEQYOQ) and

cholesterol (ID: CHOEST21) were obtained from Cambridge Crystallographic Data

Centre (CCDC) and optimized using molecular dynamics simulation with the

Gaussian 03 program. Both the optimized structures were used as a starting structure

in the docking study. AutoDock4.2 with Lamarckian Genetic Algorithm (LGA) was

used for docking study. An initial population of 150 individuals with a maximum

number of energy evaluations of 25,000,000 and a maximal number of generations of

27,000 were used as an end criterion. An elitism value of one was used and a

probability of mutation and crossing-over of 0.02 and 0.8 was used, respectively. We

have defined the conformational search space implementing an $60 \times 60 \times 60$ grid and

0.375 Å spacing between each point in such a way that it covered both the external

surface and the internal cavity of the CX6. A total of 50 docking runs were carried out.

At the end of each run, the solutions were separated into clusters according to their

lowest RMSD and the best energy score value based on an empirical free energy

function. Clustering was performed on the docked complexes with a cut-off of 2 Å.

From the docking calculations, the lowest energy conformation was selected as the

cholesterol/CX6 binding mode, and the binding free energy of the cholesterol/CX6

complex was calculated by using the semi-empirical method PM3.

Preparation of the CX6-Gra

The graphite oxide was exfoliated into graphene oxide (GO) sheets by ultrasonication

at room temperature for 1 h. The as-obtained yellow-brown aqueous suspension of

GO was stored at room temperature and used for further experiment. Compared with

the traditional procedure using highly toxic hydrazine as reductant, glucose was used

as reducing agent to reduce GO in DW. In a typical experiment, 20.0 mL of 0.5 mg

mL^{-1} GO aqueous suspension was mixed with 20.0 mL of 1.0 mg mL^{-1} CX6 aqueous

solution and the mixture was allowed to stir at room temperature for 12 h. Then, 200.0

μL of ammonia solution and 50.0 mg of glucose were added into the mixture. After

being vigorously shaken or stirred for a few minutes, the mixture was stirred at 95 ^{o}C

for 60 min. After cooling to room temperature, the resulting stable black dispersion

was centrifuged at 16000 rpm and washed with DW for 3 times. Finally, the resulting

CX6-Gra material was obtained by freeze-drying. Additionally, the Gra was prepared

with the similar procedure in the absence of CX6.

Preparation of the modified electrodes

Glass carbon electrode (GCE, 3 mm in diameter) was polished with 0.3 and 0.05 μm

Al_2O_3 powder respectively and subsequently sonicated in ethanol and DW to remove

the adsorbed substance and dried in air. The CX6-Gra was dissolved in DW at a

concentration of 1.0 mg mL^{-1} with the aid of ultrasonic agitation for 20 min, resulting

in a homogeneous suspension. To prepare the CX6-Gra modified electrode, 5 μL of

the Gra suspension was dropped onto the electrode surface and dried at room

temperature. The obtained electrode was noted as CX6-Gra/GC electrode.

Electrochemical measurements

8

DPV was applied in 0.1 M PBS (pH 7.0) from 0.1 to –0.7 V with a pulse amplitude of

0.05 V and a pulse width of 0.05 s. EIS was recorded in the frequency range from 10^{-1}

to 10^5 Hz with an amplitude of 5 mV using 2.0 mM $[Fe(CN)_6]^{3-/4-}$ redox couple (1:1)

with 0.1 M KCl as supporting electrolyte. All the measurements were carried out at

room temperature. As cholesterol has very low solubility in water, 1.0 mM stock

solution of cholesterol was prepared in ethanol and diluted to different concentrations

by 0.1 M PBS (pH 7.0) for further use. Before electrochemical measurements, the

CX6-Gra/GCE was incubated with 100 μM MB solution (in 0.1 M PBS, pH 7.0) for

30 min, and rinsed gently with DW. Then, the electrode was further incubated with

different concentrations of cholesterol solution for 30 min. After that, the electrode

was rinsed gently with DW and the current response of the MB-bound CX6-Gra/GCE

was investigated by DPV in 0.1 M PBS (pH 7.0).

Cholesterol detection in serum

Cholesterol detection in serum was performed using human serum. A stock solution of

cholesterol (1.0 mM) was prepared in ethanol and diluted to different concentrations

by 0.1 M PBS (pH 7.0) for further use. The serum sample was diluted 50 times with

0.1 M PBS (pH 7.0) and mixed with known amount of cholesterol. Next, this solution

was used to detect cholesterol according to the procedure described above.

Results and Discussion

Absorbance and fluorescence spectra analysis

The absorption spectra of MB in the presence of various concentrations of CX6 were investigated. As shown in **Fig. 1A**, MB exists a monomer/dimer equilibrium in 0.1 M PBS at pH 7.0. The absorption spectrum of MB monomer is at 654 nm and dimer is at 605 nm. Upon successive addition of CX6 (up to 20 µM), the monomer absorption band showed a systematic decrease. The dimer band decreased to reach a plateau value at high CX6 concentration. This indicated that CX6 weakened the absorbance of the MB monomer by the formation of the inclusion complex and suppressed the dimer formation. Interestingly, the addition of cholesterol to the mixture of CX6 and MB led to a successive reversion of the monomer absorption band and a significant decrease of the dimer band (**Fig. 1B**). This may be attributed to the displacement of MB by cholesterol from the CX6 host. **Fig. 1C** shows the fluorescence titrations of MB (10 µM, λex = 640 nm) upon successive addition of CX6 (up to 2.5 µM) in 0.1 M PBS at pH 7.0. The addition of CX6 caused the quenching of the fluorescence intensities of MB solutions. In contrast, a typical displacement titration is depicted in **Fig. 1D**, where the addition of cholesterol, reverts the fluorescence changes originally caused by the addition of the CX6. The competitive fluorescence titrations confirmed the displacement of MB by cholesterol from the CX6 host.

The mechanism of the competitive host–guest interaction

A double reciprocal plot of $1/(F_0-F)$ versus $1/[CX6]$ for MB to CX6 was obtained (**Fig. S1**), indicating the existence of a 1:1 complex.[5] From the plots the binding constant (K) for the 1:1 MB/CX6 complex was calculated to be $3.05\times10^5\,M^{-1}$. It was

difficult to obtain the K value of the cholesterol/CX6 complex using the same method

due to the negligible change of fluorescence intensity because cholesterol itself has no

fluorescence. In order to rationalize our experimental data and to infer the inclusion

pattern, molecular docking was performed to study the CX6/cholesterol inclusion

complex. Typically, the more negative the binding energy is, the stronger interaction

is between the host and guest molecules. As listed in **Table S1**, the lowest binding free

energy ($\triangle G$) was –8.01 kcal/mol for the host–guest complex of cholesterol and CX6

with 1:1 stoichiometry calculated by PM3 method. The K value of the

cholesterol/CX6 complex could be estimated to be $7.50 \times 10^6 \, \text{M}^{-1}$ from the following

equation: $\triangle G = -RT \ln K$, R is the gas constant and T is the experimental temperature.

The K value of cholesterol/CX6 complex was more than 20 times greater than that of

MB/CX6, which demonstrated the stronger binding of cholesterol with CX6 than that

with MB. The lowest energy docked conformation for 1:1 complex of cholesterol and

CX6, shown in **Fig. 2A**, reveals that the partial inclusion of cholesterol molecule in

the hydrophobic cavity of CX6. The cyclohexanol part and the alkyl chain of the

cholesterol molecule inserted into the cavity of CX6 host molecule. Analysis of

host–guest interaction as obtained from the docking studies reveals that hydrogen

bonding, electrostatic interactions, and hydrophobic interactions are the predominant

driving forces of the host–guest complex. Firstly, the hydroxyl on cyclohexanol of the

cholesterol molecule formed hydrogen bonding with the $-SO_3^-$ of CX6 and the bond

length is 2.0 Å. Secondly, as shown in **Fig. 2B**, strong electrostatic interactions

formed between the positive part of cholesterol molecule and the negative $-SO_3^-$ of

CX6. Thirdly, as revealed in **Fig. 2C**, strong hydrophobic interactions also formed

between the hydrophobic alkyl chain of cholesterol molecule and the CX6.

Characterization of the CX6-Gra composite

The CX6-Gra was prepared via a one-pot wet-chemical strategy based on glucose

reduction of graphene oxide in the presence of CX6. The dispersibilities of Gra and

CX6-Gra were investigated as shown in **Fig. S2**. Although the GO is highly water

soluble when it is chemically converted into Gra via glucose reduction, it forms

agglomerated Gra due to the strong π–π stacking interaction between Gra sheets and

lowering of surface hydrophilic groups originally present in GO. However, when the

GO reduction is performed in the presence of CX6, the Gra becomes highly water

soluble even after removing the free CX6 via high-speed centrifugation (16000 rpm

for 3 times) and no obvious precipitates are observed after being stored for more than

3 months.

The synthesized Gra and CX6-Gra materials were characterized by UV-vis

spectroscopy. As shown in **Fig. S3**, the GO shows a strong absorption at 230 nm and a

shoulder at 300 nm, which correspond to the π–π* transition of the aromatic C=C

bond and the n–π* transition of the C=O bond, respectively. After reduction, the peak

at 230 nm gradually redshifts to 260 nm, suggesting that the electronic conjugation

within the Gra sheets is restored upon glucose reduction. [10,24,25]

Raman spectroscopy is one of the most widely used techniques to characterize the

structural and electronic properties of Gra including disordered and defective

structures, defect density, and doping levels. **Fig. S4** shows the typical Raman spectra

of GO, Gra and CX6-Gra. As expected, GO displays two prominent peaks at 1340 and

1584 cm^{-1} corresponding to the D and G bands, respectively. The Gra shows two

prominent peaks at 1347 and 1586 cm^{-1}, corresponding to the breathing mode of

k-point phonons of A_{1g} symmetry (D band) and the E_{2g} phonons of C sp^2 atoms (G

band) of Gra, respectively. The intensity ratio of the D band to the G band (I_D/I_G) is

clearly higher when compared with that of GO (0.98 vs. 0.77), suggesting a decrease

in sp^2 domains and a partially ordered crystal structure of Gra induced by glucose

reduction. The Raman spectra of CX6-Gra was similar to Gra, indicating that the

crystal structure of Gra is not severely affected by CX6.

The microstructure of the CX6-Gra was characterized by SEM (**Fig. S5**) and TEM

(**Fig. S6**) observation. The SEM and TEM images reveal that the CX6-Gra material

consists of randomly aggregated thin, wrinkled sheets closely associated with each

other. Since it is difficult to distinguish the CX6 molecules on the SEM and TEM

images, the Gra and CX6-Gra materials were further characterized by FTIR and TGA

analysis.

The synthesized Gra and CX6-Gra materials were characterized by FTIR as

shown in **Fig. S7**, by comparing FTIR spectra of CX6, CX6-Gra, and Gra, significant

features can be observed: Firstly, the peaks for $-SO_3^-$ at 1160 and 1040 cm^{-1}, as seen

in the spectra of pure CX6, also appeared in the spectra of CX6-Gra, indicating that

CX6 was attached to the surface of Gra. [16] Secondly, the alteration of the peak value

at 3391 cm^{-1} of –OH in CX6 stretching vibrations shifting to 3360 cm^{-1} in CX6-Gra

13

was identified as a result of hydrogen interactions between the remaining

oxygen-containing groups of Gra and hydroxyl groups of CX6. [10] In addition, it has

been reported that the composites of calixarenes and carbon materials (e.g. carbon

nanotube, Gra) could be formed by $\pi-\pi$ interactions and hydrogen interactions. [16,19−21]

These results demonstrated that CX6 had successfully self-assembled to Gra and

formed CX6-Gra nanocomposite.

The prepared CX6-Gra and the related materials were also characterized by TGA,

as shown in **Fig. S8**. The GO curve shows a small mass loss (20%) at approximately

160 °C and a major mass loss (50%) at approximately 300 °C owing to the loss of

adsorbed water and pyrolysis of the labile oxygen-containing functional groups,

respectively. In contrast, the Gra is more thermally stable than GO. After reduction,

the mass loss is 24% compared to the 62% mass loss at 600 °C for GO. For the

pristine Gra, the minor loss in mass (24%) at a temperature of approximately 600 °C

was due to the pyrolysis of a very small amount of the remaining oxygen-containing

functional groups. The CX6-Gra material exhibited an abrupt mass loss when the

temperature was approximately 450 °C because of the decomposition of CX6; the

mass loss reached about 42 wt% when the temperature was 600 °C. The amount of

CX6 molecules grafted to Gra was estimated to be 18.0 wt%. This results was in

accordance with previous study. [16]

Design strategy of the electrochemical sensor

The design strategy of the proposed electrochemical sensor based on the competitive

host–guest interaction between CX6 and MB (signal probe)/cholesterol (target) was

illustrated in **Scheme 1**. MB molecules can enter into the inner cavity of CX6 due to

the host–guest interaction, and the MB-bound CX6-Gra/GCE displays a remarkable

reduction peak due to MB. However, in the presence of cholesterol, competitive

association to the CX6 occurs and the MB molecules are displaced by cholesterol

molecule. This results in a decrease of the reduction peak current of the MB probe.

Feasibility of the electrochemical sensor

To demonstrate the assay feasibility of the proposed competitive electrochemical

sensing platform, DPV response of the CX6-Gra/GCE was investigated in 0.1 M pH

7.0 PBS. As can be seen from **Fig. 4A**, no detectable signal (**curve a**) is observed for

the CX6-Gra/GCE in 0.1 M pH 7.0 PBS due to the absence of the redox mediator MB.

After incubated in 100 μM MB solution for 30 min, the MB-bound CX6-Gra/GCE

was then tested in 0.1 M pH 7.0 PBS and an obvious reduction peak of MB (**curve b**)

can be observed at about –0.3 V. When the CX6-Gra/GCE was first incubated in 100

μM MB solution for 30 min and further incubated in 25 μM cholesterol solution for

30 min, then tested in 0.1 M pH 7.0 PBS, a decreased reduction peak (**curve c**) was

obtained due to competitive association of cholesterol/MB to the CX6 occurs. This is

because cholesterol has higher binding affinity to CX6 cavity due to its hydrophobic

nature. This suggests that the MB molecules present inside the CX6-Gra/GCE host

can be replaced by cholesterol and the MB-bound CX6-Gra/GCE can be used to

sensitively detect cholesterol by the competitive electrochemical sensing strategy

shown in **Scheme 1**.

Electrochemical characterization of the modified electrodes

EIS was performed at the potential of 0.1 V and the frequency ranges was from 10^{-1} to

10^5 Hz, using 2.0 mM $[Fe(CN)_6]^{3-/4-}$ redox couple (1:1) with 0.1 M KCl as supporting

electrolyte. The value of the charge transfer resistance (R_{ct}) of the modified electrode

was estimated by the semicircle diameter. **Fig. S9** illustrates the EIS of the bare GCE,

Gra/GCE, and CX6-Gra/GCE. Obviously, the bare GCE exhibited a semicircle

portion and the value of R_{ct} was estimated to be approximately 800 Ω. While the R_{ct}

decreased dramatically, nearly to zero at Gra/GCE, indicating that Gra/GCE formed

high electron conduction pathways between the electrode and electrolyte, and had

good conductivity and improved obviously the diffusion of ferricyanide toward the

electrode interface. When the CX6-Gra modified on the bare GCE, the semicircle

increased to 1500 Ω, this is because of CX6 layer hindered the electron transfer and

made the interfacial charge transfer difficult, suggesting that CX6 molecules were

successfully immobilized on the surface of Gra. This result is in accordance with that

of TGA of mass loss. A modified Randle's equivalent circuit was provided in **Fig. 3**

(inset). The impedance data were fitted with commercial software Zview2. The fitting

curves were obtained by the equivalent circuit depicted in **Fig. 3**. A good fit was

obtained with the model used for all experimental data. The semicircle portion (R_{ct}),

observed at higher frequencies in **Fig. 3**, corresponding to the

electron-transfer-limited process, whereas the linear part was the characteristics of the

16

lower frequencies range and represented the diffusion-limited electron transfer

process. The simulated values of the equivalent circuit elements were summarized in

Table 1, where it showed that the change of R_{ct} was rather significant. The changes in

R_{ct} were much larger than those in other impedance elements from **Table1**, therefore,

the R_{ct} was considered as a suitable signal for expressing the interfacial properties of

the as prepared electrode. A constant phase element (CPE) was used instead of the

classical capacitance to fit the impedance data. R_s was the ohmic resistance of the

electrolyte solution. Z_w was the Warburg impedance, resulting from the diffusion of

ions from the electrolyte to the electrode interface. [26]

Quantitative analysis of cholesterol

Under optimal conditions (the incubation time of the CX6-Gra/GCE in MB solution

and the MB-bound CX6-Gra/GCE in cholesterol solution was studied, which was

provided in Supporting Information), DPV was used to determine the concentrations

of cholesterol because it is a highly sensitive and low-detection limit electrochemical

method. **Fig. 4B** shows the DPV curves of electrochemical signal on the MB-bound

CX6-Gra/GCE under different concentrations of cholesterol solution. The reduction

peak currents of MB decreased with the increased cholesterol concentrations. Above

50 µM, the signal reached its saturation. Here, the remaining signal should be that of

the nonspecific adsorption of MB caused by the π−π interactions between MB and

Gra. However, these will not make difference to the DPV results, as MB remains

intact on the surface of Gra in the beginning as well as at the end of the experiment. A

17

control experiment was carried out to exclude the possibility of desorption of MB

from the Gra surface during cholesterol detection (**Fig. S12**). **Fig. 4C** shows the

corresponding calibration curve for cholesterol quantification. The peak currents

changes were proportional to the cholesterol concentrations between 0.50 and 50.00

µM with a detection limit of 0.20 µM (*S/N*=3). The corresponding regression equation

was calculated as ΔI (µA) = 0.099C (µM) + 0.469 with correlation coefficients of

0.996. The sensitivity was obtained from the slope of the calibration plot and was

0.099 µA µM^{-1}. Detection limit was less than 1.0 µM which was quite low and

satisfactory with respect to other recently reported articles. **Table 2** illustrates few of

the recent literatures on cholesterol sensing platforms, through both enzymatic and

non-enzymatic sensing routes. The detection limit and sensitivity of the present

sensing strategy is comparatively better than the reported ones.

Selectivity

As we know, human blood serum contains many more biocomponents like salts,

amino acids, carbohydrates, lipids etc., those can interfere with cholesterol detection

and hamper the selectivity of the electrochemical sensor. Therefore, we have tested

interference from common molecules present in human blood serum and found very

negligible interference. As shown in **Fig. 4D**, some salts, carbohydrates, protein,

anionic surfactant, etc. including glucose, sucrose, ascorbic acid (AA), bovine serum

albumin (BSA), sodium dodecyl sulphate (SDS), Tween 20, NaCl, KCl, and, MgCl$_2$

showed negligible interference even at the concentration of 2.0 mM, compared to

18

cholesterol detected for only 50 µM concentration. In addition, several analogues of

cholesterol including corticosterone, estrone, β-estradiol, and β-sitosterol were also

used for the interference study. The results indicated that corticosterone and estrone

exhibited weak interference while β-estradiol and β-sitosterol produced serious

interference. This was ascribed to the similar structures of β-estradiol, β-sitosterol and

cholesterol. The reproducibility and stability of the sensor were also studied and

supplied in Supporting Information.

Real sample analysis

The proposed method was used to detect cholesterol in serum samples using standard

addition methods to evaluate the feasibility of the MB-bound CX6-Gra/GCE for real

sample analysis. The serum sample was diluted fifty times with 0.1 M pH 7.0 PBS.

Results showed recoveries ranging from 99.0% to 104.4% and RSDs ranging from

2.45% to 4.32% (**Table 3**). The results demonstrated that this method can be extended

for cholesterol detection in blood. Although the 2.0 mM of β-estradiol and β-sitosterol

seriously interfere with the detection of cholesterol (50 µM), the cholesterol detection

in human serum was also very successful. This may be due to the very low

concentration of β-estradiol in human plasma. [34] Serum β-estradiol levels vary over a

range from 41 to 272 pg mL^{-1} during the menstrual cycle in premenopausal women,

and the β-estradiol levels decrease to about 4–14 pg mL^{-1} after menopause. [35] In the

case of β-sitosterol, it mainly exists in plants. The proposed sensing platform may also

be expanded to wide and potential applications in biological samples. It is worthy to

note that the CX6 is more stable than cholesterol selective enzymes (mostly oxidase)

under complex conditions. Thus, the present sensing platform seems to be more

suitable for analysis of practical cholesterol samples than traditional enzyme-based

biosensor.

Conclusions

In summary, a sensitive and selective electrochemical approach for cholesterol

sensing based on a competitive host-guest interaction between CX6 and signal

probe/target molecules using CX6-Gra-modified electrode was developed. Due to the

good electron transfer property of the Gra and the excellent host–guest recognition of

CX6, the developed CX6-Gra/GCE displays excellent analytical performance for the

electrochemical detection of cholesterol: the linear response range is 0.50–50.00 μM

and the LOD is 0.20 μM (*S/N*=3). In addition, the developed electrochemical sensing

platform is important as it does not use any enzyme or antibody for detection of

cholesterol efficiently and selectively over the common interfering species. Molecular

modeling calculations revealed that the complexation of cholesterol and CX6 could

reduce the energy of the system and the complex of 1:1 host–guest stoichiometry had

the lowest ΔG value of –8.01 kcal/mol. The molecular docking studies suggested that

hydrogen bonding, electrostatic interactions, and hydrophobic interactions should be

the predominant driving forces for the formation of the inclusion complex.

Notes and references

1   F. Biedermann, V. D. Uzunova, O. A. Scherman, W. M. Nau, A. D. Simone, *J. Am. Chem. Soc.*, 2012, **134**, 15318−15323.

2   F. Biedermann, M. Vendruscolo, O. A. Scherman, A. D. Simone, W. M. Nau, *J. Am. Chem. Soc.*, 2013, **135**, 14879−14888.

3   G. Ghale, W. M. Nau, *Acc. Chem. Res.*, 2014, **47**, 2150−2159.

4   F. Biedermann, W. M. Nau, *Angew. Chem. Int. Ed.*, 2014, **53**, 5694–5699.

5   C. F. Li, J. X. Feng, H. X. Ju, *Analyst*, 2015, **140**, 230–235.

6   A. Praetorius, D. M. Bailey, T. Schwarzlose, W. M. Nau, *Org. Lett.*, 2008, **10**, 4089−4092.

7   G. Ghale, V. Ramalingam, A. R. Urbach, W. M. Nau, *J. Am. Chem. Soc.*, 2011, **133**, 7528–7535.

8   J. M. Chinai, A. B. Taylor, L. M. Ryno, N. D. Hargreaves, C. A. Morris, P. John Hart, A. R. Urbach, *J. Am. Chem. Soc.*, 2011, **133**, 8810–8813.

9   A. Mondal, N. R. Jana, *Chem. Commun.*, 2012, **48**, 7316–7318.

10   X. Mao, D. Tian, H. Li, *Chem. Commun.*, 2012, **48**, 4851−4853.

11   G. B. Zhu, L. Wu, X. Zhang, W. Liu, X. H. Zhang, J. H. Chen, *Chem. Eur. J.*, 2013, **19**, 6368–6373.

12 N. Agnihotri, A. D. Chowdhury, A. De, *Biosens. Bioelectron.*, 2015, **63**, 212–217.

13 X. Zhang, L. Wu, J. W. Zhou, X. H. Zhang, J. H. Chen, *J. Electroanal. Chem.*, 2015, **742**, 97–103.

14 L. Mutihac, J. H. Lee, J. S. Kim, J. Vicens, *Chem. Soc. Rev.*, 2011, **40**, 2777–2796.

15 R. N. Dsouza, U. Pischel, W. M. Nau, *Chem. Rev.*, 2011, **111**, 7941–7980.

16 J. Zhou, M. Chen, G. W. Diao, *ACS Appl. Mater. Interfaces*, 2013, **5**, 828−836.

17 D. Chen, L. H. Tang, J. H. Li, *Chem. Soc. Rev.*, 2010, **39**, 3157–3180.

18 D. R. Dreyer, S. Park, W. C. Bielawski, R. S. Ruoff, *Chem. Soc. Rev.*, 2010, **39**, 228–240.

19 X. J. Chen, R. A. Boulos, P. K. Eggers, C. L. Raston, *Chem. Commun.*, 2012, **48**, 11407–11409.

20 E. Eroglu, W. Z. Zang, P. K. Eggers, X. J. Chen, R. A. Boulos, M. Haniff Wahid, S. M. Smith, C. L. Raston, *Chem. Commun.*, 2013, **49**, 8172−8174.

21 X. J. Chen, C. T. Gibson, J. Britton, P. K. Eggers, M. Haniff Wahid, C. L. Raston, *Chem. Commun.*, 2015, **51**, 2399−2402.

22 N. Batra, M. Tomar, V. Gupta, *Biosens. Bioelectron.*, 2015, **67**, 263–271.

23 J. Motonaka, L. R. Faulkner, *Anal. Chem.*, 1993, **65**, 3258–3261.

24 Y. Guo, S. Guo, J. Ren, Y. Zhai, S. Dong, E. Wang, *ACS Nano*, 2010, **4**, 4001−4010.

25 C. Z. Zhu, S. J. Guo, Y. X. Fang, S. J. Dong, *ACS Nano*, 2010, **4**, 2429−2437.

26   A.J. Bard, L.R. Faulkner, Electrochemical Methods: Fundamentals and

Applications, second ed., Wiley, New York, 2001 .

27   L. Zhu, L. Xu, L. Tan, H. Tan, S. Yang, S. Yao, *Talanta*, 2013, **106**, 192–199.

28   C. Z. Zhao, L. Wan, L. Jiang, Q. Wang, K. Jiao, *Anal. Biochem.*, 2008, **383**,

25–30.

29   N. Ruecha, R. Rangkupan, N. Rodthongkum, O. Chailapakul, *Biosens.*

Bioelectron., 2014, **52**, 13–19.

30   A. Ahmadalinezhad, A. C. Chen, *Biosens. Bioelectron.*, 2011, **26**, 4508–4513.

31   A. K. Giri, A. Sinhamahapatra, S. Prakash, J. Chaudhari, V. K. Shahi, A. B.

Panda, *J. Mater. Chem. A*, 2013, **1**, 814–822.

32   A. Umar, R. Ahmad, S. W. Hwang, S. H. Kim, A. Al-Hajry, Y. B. Hahn,

Electrochim. Acta, 2014, **135**, 396–403.

33   U. Saxena, M. Chakraborty, P. Goswami, *Biosens. Bioelectron.*, 2011, **26**,

3037–3043.

34   M. J. Monerris, F. J. Arévalo, H. Fernández, M. A. Zon, P. G. Molina, *Sens.*

Actuators B, 2015, **208**, 525–531.

35   T.-B. Xin, H. Chen, Z. Lin, S.-X. Liang, J.-M. Lin, *Talanta*, 2010, **82**,

1472–1477.

Figure captions:

Fig. 1. (A) Absorbance spectra of MB (10 μM) upon successive addition of CX6 (up

to 20 µM) in 0.1 M PBS at pH 7.0; **(B)** Absorbance spectra for the competitive

displacement of MB (10 µM) from CX6 (20 µM) by cholesterol (up to 20 µM) in 0.1

M PBS at pH 7.0; **(C)** Fluorescence titrations of MB (10 µM, λex = 640 nm) upon

successive addition of CX6 (up to 2.5 µM) in 0.1 M PBS at pH 7.0; **(D)** Fluorescence

titration for the competitive displacement of MB (10 µM) from CX6 (2.5 µM) by

cholesterol (up to 5.0 µM) in 0.1 M PBS at pH 7.0.

Fig. 2. (A) Lowest energy cholesterol/CX6 docked complex for 1:1 host–guest

stoichiometry (left is the side view, right is the top view); The electrostatic forces (**B**,

left is the top view of CX6, right is the top view of cholesterol/CX6 complex; red

represents the strongest positively charged, blue represents the strongest negatively

charged) and hydrophobic forces (**C**, left is the top view of CX6, right is the top view

of cholesterol/CX6 complex; brown represents the strongest hydrophobic, blue

represents the strongest hydrophilic) of cholesterol/CX6 docked complex for 1:1

host–guest stoichiometry.

Scheme 1. Competitive host–guest molecular recognition of cholesterol (Cho) using

CX6-Gra against MB.

Fig. 3. Nyquist diagram of the fitting curves compared with the experimental results.

Inset: Randle's equivalent circuit corresponding to the impedance features.

24

1
2
3
4
5
6
7
8
9
10
11
12
13
14
15
16
17
18
19
20
21
22
23
24
25
26
27
28
29
30
31
32
33
34
35
36
37
38
39
40
41
42
43
44
45
46
47
48
49
50
51
52
53
54
55
56
57
58
59
60

Fig. 4. (A) DPV response of the CX6-Gra/GCE in 0.1 M pH 7.0 PBS **(a)**; DPV

response of the CX6-Gra/GCE incubated in 100 μM MB solution for 30 min and then

tested in 0.1 M pH 7.0 PBS **(b)**; DPV response of the CX6-Gra/GCE incubated in 100

μM MB solution for 30 min and further incubated in 25 μM cholesterol solution for

30 min and then tested in 0.1 M pH 7.0 PBS **(c)**. **(B)** DPV curves of the proposed

sensing platform under different concentrations of cholesterol. **(C)** Calibration curves

for the determination of cholesterol using the proposed sensor. The error bars

represent the standard deviations of three parallel tests. **(D)** Interference studies using

different species in the developed cholesterol detection method, using DPV and

keeping all the parameters constant. The cholesterol concentration was 50 μM against

the concentration of all other substances, which was kept at 2.0 mM.

Analyst Accepted Manuscript

Table 1

Simulated values of the equivalent circuit elements for the bare GC, Gra/GC, and CX6-Gra/GC electrodes.

Electrode	R_s (Ω)	CPE (F)	R_{ct} (Ω)	Z_w (Ω)
GCE	101.4	2.5E-06	805	0.28
Gra/GCE	132.0	1.1E-06	96.3	0.32
CX6-Gra/GCE	102.8	3.4E-06	1495	0.31

Table 2

Comparison of the present work with other recent literatures, using various electrode or matrix for cholesterol sensing.

Electrode or Matrix	Method	Liner range (μM)	LOD (μM)	Ref
Nafion/ChOx/GNPs-MWCNTs/GCE	DPV	10.0–5000.0	4.3	27
Chit–Hb/Chit–ChOx	amperometry	10.0–600.0	9.5	28
ChEt–ChOx/ZnO–CuO/ITO/glass	CV	500.0–12000.0	500.0	22
ChOx/PANI/PVP/Graphene	amperometry	50.0–10000.0	1.0	29
ChOx/Nano-ZnO/ITO	CV	130.0–10360.0	13.0	30
ChOx/ZnO(T)/CT/GCE	CV	400.0–4000.0	200.0	31
Nafion/ChOx/Fe_2O_3	CV	100.0–8000.0	18.0	32
AuE/Dithiol/AuNPs/MUA/ChOx	CV	40.0–220.0	34.6	33
Grp/β-CD/Methylene Blue	DPV	1.0–100.0	1.0	12
Grp/β-CD/Rhodamine 6G	Fluorescence	5.0–30.0	5.0	9
CX6-Gra/GCE	DPV	0.5–50.0	0.20	This work

Table 3

Determination of cholesterol in human serum samples (n=3).

Sample	Added (μM)	Founded (μM)	RSD (%)	Recovery (%)
1	5.0	4.95±0.22	4.32	99.0
2	10.0	10.22±0.35	3.51	102.2
3	20.0	20.08±0.54	2.45	104.4

26

Figures:

Fig. 1.

Yang et al.

(A)

(B)

(C)

Fig. 2.

Yang et al.

MB-bound CX6-Gra (a)   Cho-bound CX6-Gra (b)
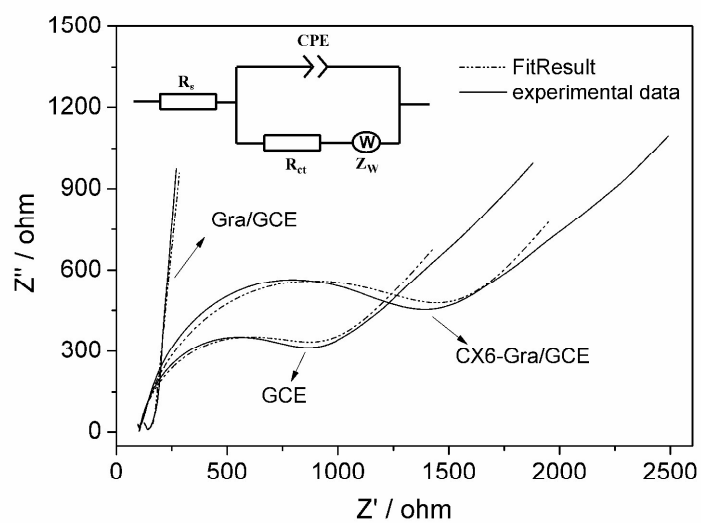
DPV response decrease
upon competitor addition
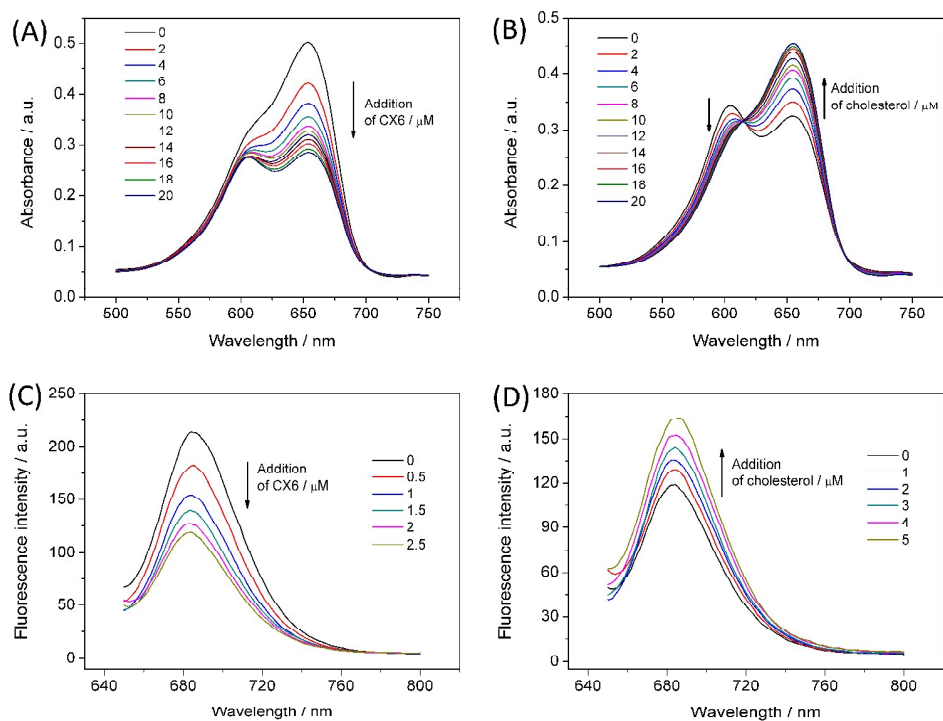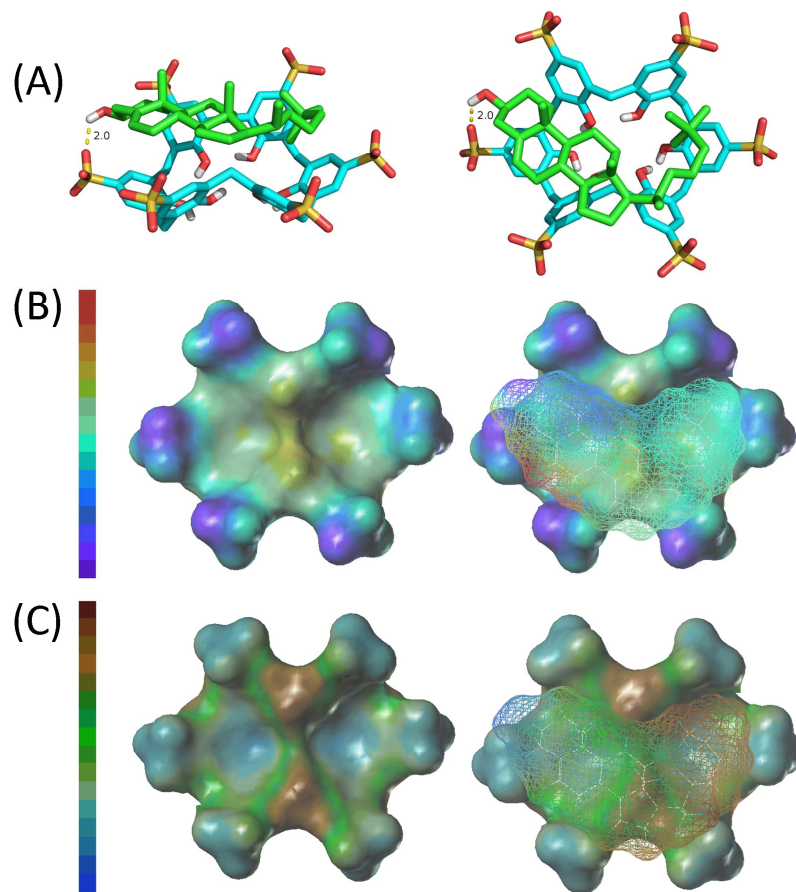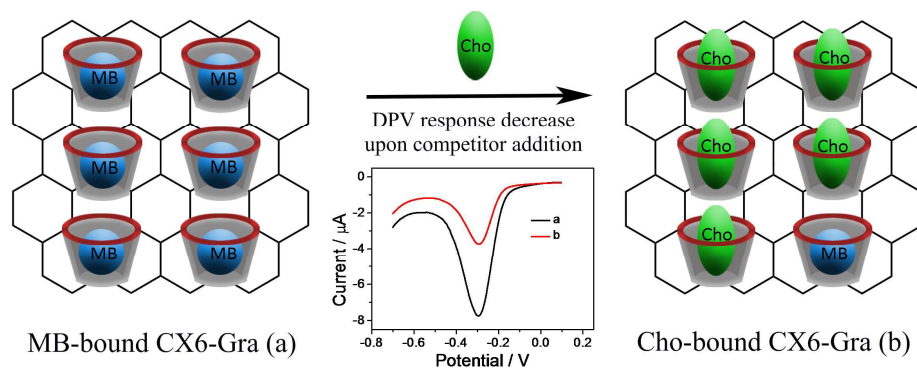
Scheme 1.

Yang et al.

Fig. 3.

Yang et al.

Fig. 4.

Yang et al.